

TOU Optimization Model of Microgrid Based on Demand Side Response and Economical Operation

Xiaohong Lv, Qian Li, Bin Wang, Min Zhang, Dejian Wang, Wenzhong Cao

State Grid Chongqing Electric Power Company

Chongqing, China

Abstract—This paper studies the user response characteristic to the time of use price, and establishes the user load response characteristic curve to the time of use price on the basis of consumer psychology. Based on the optimal operation model, the paper analyses the effect of demand side. The paper establishes the optimal TOU model based on economic operation and the demand side response. The power supply enterprise benefit maximization is the goal in this model, the best time of use price and optimal scheduling scheme can be made according to the prediction of the load. The model can be used to formulate the best scheme of TOU in a given time period, and provides a quantitative basis for electricity pricing of microgrid. Example analysis results show that the operation cost of microgrid reduces and the power supply enterprise benefit increases when considering the demand side response, the model has important guiding significance on the formulation of grid electricity price and scheduling scheme.

Keywords—*microgrid; economical operation; demand side response; time-of-use price*

I. INTRODUCTION

With the development of power industry, smart grid attracts more and more attention. Due to load fluctuation, grid investment increases and energy is wasted. To save grid investment cost and increase energy utilization rate, TOU was proposed to guide users to adjust electricity consumption structure and smooth the load shifting curve from peak to valley.

Researches on microgrid mainly include microgrid planning and operation. For microgrid operation, attentions were mainly paid to the economic dispatch. Although some researches on economical operation of microgrid have been reported, few of them explored effect of demand side response. Reference [1,2] studied user response to TOU based on consumer psychology. Reference [3] established a TOU model for power stations according to their different coal consumption characteristics. Reference [4] studied the response behavior of TOU to load, established a model for optimization management of micro power source and demand side load, and analyzed effect of demand side response to the economical operation of microgrid. Other existing studied were mainly from the perspective of cost and took microgrid into con-

sideration [5-7]. However, the established model didn't take user benefit into account. Few of the existing researchers analyzed effect of demand side response on the economical operation of microgrid and optimized TOU of microgrid from the perspective of economical operation.

Based on existing researches and consumer psychology, this paper established a load response characteristic model and discussed effect of TOU on the economical operation of microgrid. To maximize total revenues of power supply enterprises, a TOU optimization model of microgrid was established based on demand side response and economical operation. This model can be used to make optimal TOU and corresponding optimal generation scheduling of microgrid.

II. DEMAND RESPONSE ANALYSIS BASED ON TOU

Consumers often choose the best time to purchase according to commodity price changes. When adopting TOU (Time of Use Price), consumers will change traditional electricity consumption structure. They may reduce electricity consumption at peak with higher price, but increase electricity consumption at valley with lower price. In this way, some loads at peak are shifted to valley period. Such user responses to electricity price generally can be reflected by the load shifting curve. Based on existing researches, the load curve under TOU was determined based on the principle of consumer psychology.

Based on the principle of consumer psychology, different commodity prices will receive different consumer responses. When the external stimulate is smaller than the minimum level, users make no response. As the external stimulate succeeds the maximum level, user response become stable. Under this circumstance, user response is uncorrelated with the stimulate degree. When minimum level < external stimulate < maximum level, user response increases with the increase of stimulates. Hence, the concept of load shifting rate was introduced. Load shifting rate is equal to the ratio of shifted loads from peak to valley and loads at peak after the implementation of TOU. Abundant survey results demonstrate that load shifting rate and electricity price difference can be expressed by piecewise linear function approximately [8].

A. Loading shifting rate from peak to valley

Adopted TOU, some users shift some loads from peak to valley. The load shifting rate from peak to valley is expressed by equation (1) and the corresponding load shifting curve is shown in Fig .1.

$$\lambda_{pv} = \begin{cases} 0 & (0 \leq \Delta p_{pv} < a_{pv}) \\ K_{pv}(\Delta p_{pv} - a_{pv}) & (a_{pv} \leq \Delta p_{pv} < b_{pv}) \\ \lambda_{pv}^{\max} & (\Delta p_{pv} \geq b_{pv}) \end{cases} \quad (1)$$

where Δp_{pv} is the electricity price difference between peak and valley, $\Delta p_{pv} = p_p - p_v$ (p_p is electricity price at peak and p_v is electricity price at valley); a_{pv} is the minimum load shifting from peak to valley (break point of dead zone); b_{pv} is the maximum load shifting from peak to valley (break point of saturation zone); K_{pv} is the slope of linear zone; λ_{pv}^{\max} is the maximum load shifting rate from peak to valley.

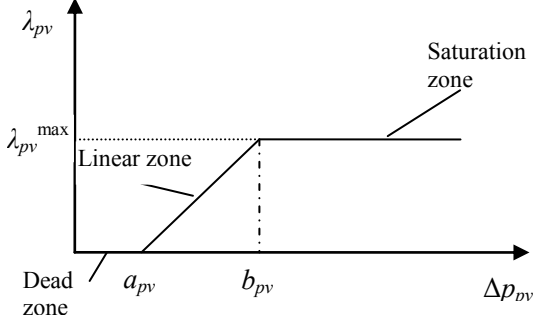


Figure 1. Load shifting curve from peak to valley

B. Load shifting rate from flat to valley

The load shifting rate from flat to valley is expressed by equation (2) and the corresponding load shifting curve is shown in Fig .2.

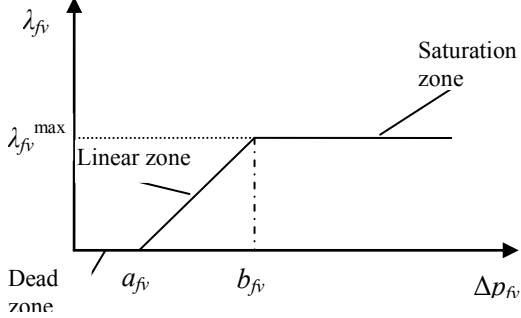


Figure 2. Load shifting curve from flat to valley

$$\lambda_{fv} = \begin{cases} 0 & (0 \leq \Delta p_{fv} < a_{fv}) \\ K_{fv}(\Delta p_{fv} - a_{fv}) & (a_{fv} \leq \Delta p_{fv} < b_{fv}) \\ \lambda_{fv}^{\max} & (\Delta p_{fv} \geq b_{fv}) \end{cases} \quad (2)$$

where Δp_{fv} is the electricity price difference between flat and valley, $\Delta p_{fv} = p_f - p_v$ (p_f is electricity price at flat); a_{fv} is the minimum load shifting from flat to valley (break point of dead zone); b_{fv} is the maximum load shifting from flat to valley (break point of saturation zone); K_{fv} is the slope of linear zone; λ_{fv}^{\max} is the maximum load shifting rate from flat to valley.

C. Load shifting rate from peak to flat

The load shifting rate from peak to flat is expressed by equation (3) and the corresponding load shifting curve

is shown in Fig .3.

$$\lambda_{pf} = \begin{cases} 0 & (0 \leq \Delta p_{pf} < a_{pf}) \\ K_{pf}(\Delta p_{pf} - a_{pf}) & (a_{pf} \leq \Delta p_{pf} < b_{pf}) \\ \lambda_{pf}^{\max} & (\Delta p_{pf} \geq b_{pf}) \end{cases} \quad (3)$$

where Δp_{pf} is the electricity price difference between peak and flat, $\Delta p_{pf} = p_p - p_f$; a_{pf} is the minimum load shifting from peak to flat (break point of dead zone); b_{pf} is the maximum load shifting from peak to flat (break point of saturation zone); K_{pf} is the slope of linear zone; λ_{pf}^{\max} is the maximum load shifting rate from peak to flat.

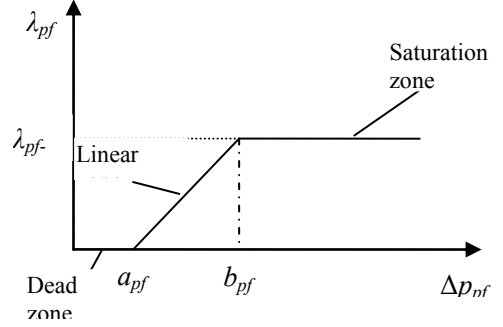


Figure 3. Load shifting curve from peak to flat

TOU causes load shifting. Express load shifting rate under different electricity price by above mentioned piecewise linearity curve. The fitting loads of different periods are:

$$L_t = \begin{cases} L_{t0} + \lambda_{pv} \cdot \bar{L}_p + \lambda_{fv} \cdot \bar{L}_f & t \in T_v \\ L_{t0} + \lambda_{pf} \cdot \bar{L}_p - \lambda_{fv} \cdot \bar{L}_f & t \in T_f \\ L_{t0} - \lambda_{pv} \cdot \bar{L}_p - \lambda_{pf} \cdot \bar{L}_p & t \in T_p \end{cases} \quad (4)$$

where L_{t0} is forecasted load in t before the implementation of TOU; L_t is the forecasted load in t after the implementation of TOU; T_v , T_f and T_p are periods of valley, flat and peak, respectively; \bar{L}_v , \bar{L}_f and \bar{L}_p are the mean load of valley, flat and peak before the implementation of TOU.

III. EFFECT OF DEMAND RESPONSE AND MICROGRID OPERATION ON ELECTRICITY PRICE

TOU will stimulate users to adjust electricity consumption structure. To ensure balance of electric power and energy of microgrid, output of micro power sources will be adjusted according to the changes of load shifting curve. As a result, microgrid dispatching can be controlled by adjusting electricity prices. Considering the demand side response, the optimal TOU can be determined according to the optimal economic analysis.

Load and electricity price can be expressed as:

$$P_D = f_1(p) \quad (5)$$

where p is an electricity price variable; f_1 is relationship between electricity price and load (See in Section II); and P_D is load.

Load shifting curve is closely related with the operating cost of microgrid:

$$C = f_2(P_D) \quad (6)$$

where f_2 is the relationship between load and operating cost of microgrid, and C is the operating cost of microgrid.

Based on equation (5) and (6), the relationship among electricity price, load and economical operation can be established. The TOU plan accompanied with optimal economical operation of microgrid is the optimal TOU.

IV. TOU OPTIMIZATION MODEL BASED ON DEMAND SIDE RESPONSE AND ECONOMICAL OPERATION

A. Service life loss model of lead-acid battery

The service life of lead-acid battery is determined by various factors, such as service temperature, maximum charging current and charge-discharge process. Among them, the service temperature and maximum charging current are generally related with the heat dissipation and control system of the lead-acid battery. This paper focused on studying effect of charge-discharge process on the service life of lead-acid battery.

When the depth of charge-discharge cycles of the lead-acid battery is R , the maximum charge-discharge cycles before failure (N_{ESS}) are:

$$N_{ESS} = \alpha_1 + \alpha_2 e^{\alpha_3 R} + \alpha_4 e^{\alpha_5 R} \quad (7)$$

Where $\alpha_1 \sim \alpha_5$ are characteristic parameters of the lead-acid battery, which can be acquired from service life test data provided by the manufacturer.

In one charge-discharge cycle of lead-acid battery, the proportion of service life loss in the total service life is $1/N_{ESS}$ and the equivalent economic loss cost (C_1) is:

$$C_1 = C_{\text{initial-bat}} / N_{ESS} \quad (8)$$

where $C_{\text{initial-bat}}$ is the investment cost of the lead-acid battery.

During microgrid operation, the service life loss cost of the lead-acid battery in one dispatching cycle (C_{bat}) is:

$$C_{\text{bat}} = \sum_{j=0}^{N_T} C_{1,j} \quad (9)$$

where N_T is the charges and discharges of the lead-acid battery in the microgrid dispatching cycle and $C_{1,j}$ is the service life loss cost when the depth of j^{th} charge-discharge cycle is R_j .

B. Objective function

Loads shift from peak to flat or valley after the implementation of TOU, which changes the load shifting curve of the whole power system. Consequently, operating cost and selling cost may change. To explore effect of TOU on the economical operation of microgrid, an economical operation model involving demand side response was established. It aims to maximize revenues of power supply enterprises:

$$\max C_{\text{benefit}} = \sum_{t=1}^T C_{\text{sale},t} \cdot P_{Dt} \Delta t - C_{\text{total}} \quad (10)$$

where C_{benefit} is the total revenue; $C_{\text{sale},t}$ is the selling price of electricity of power supply enterprises (purchase price of users); T is the total periods in the dispatching cycle (In this paper, the dispatching cycle is one day, divided

into 24 periods); P_{Dt} is the forecasted load in t after the implementation of TOU; Δt is the interval between two periods; and C_{total} is the total operating cost of microgrid.

Calculation of C_{total} is closely related with the microgrid operation. A bi-objective TOU optimization model was established. The high-level objective is to minimize the total revenue of power supply enterprises, while the low-level objective is to minimize C_{total} under fixed loads. The lower-level objective function is:

$$\min C_{\text{total}} = \sum_{t=1}^T \left(\sum_{n=1}^N C_n^t (1 - u_{n,t-1}) u_{n,t} + \sum_{n=1}^N u_{n,t} F_{FC,m} \right) + C_{\text{bat}} \quad (11)$$

$$C_n^t = \sigma_n + \delta_n (1 - e^{(-T_m^{\text{OFF}} / \tau_n)}) \quad (12)$$

where C_n^t is the operating cost of conventional unit n (microturbine) in t ; N is the amount of conventional units; $u_{n,t}$ is the on-off state variable of n in t (1=on; 0=off); $F_{FC,m}$ is the fuel consumption cost of n in t ; C_{bat} is service life loss cost of the lead-acid battery; σ_n , δ_n and τ_n are start-up cost coefficients of n ; T_m^{OFF} is the idle time of n in t .

C. Constraints

Constraints of the TOU optimization model based on demand side response and economical operation include:

1) Purchasing cost of users

To get user supports, the TOU policy shall ensure that the purchasing cost of users won't increase.

$$M_0 \geq M_1 \quad (13)$$

where M_0 and M_1 are purchasing costs of users before and after the implementation of TOU. They are the product of electricity consumption and purchase price.

2) Electricity consumption

Total electricity consumption of users after the implementation of TOU remains same or increases slightly. This paper supposed that the total electricity consumption of users after the implementation of TOU remains the same.

$$\sum_{t \in T_p} Q_{p,t} + \sum_{t \in T_f} Q_{f,t} + \sum_{t \in T_v} Q_{v,t} = \sum_{t \in T} Q_t \quad (14)$$

$$T_p + T_f + T_v = T \quad (15)$$

where $Q_{p,t}$, $Q_{f,t}$ and $Q_{v,t}$ are electricity consumptions of peak, flat and valley in t after the implementation of TOU; Q_t is electricity consumption in t before the implementation of TOU.

3) Electricity price

$$P_p > P_f > P_v \quad (16)$$

$$2 \leq \frac{P_p}{P_v} \leq 5 \quad (17)$$

Currently, the electricity price at peak/electricity price at valley ranges between $2 \sim 5$ ^{[3][2]}.

4) Economical operation of microgrid

Constraints of economical operation include:

a) Power balance

$$\sum_{n=1}^N P_{nt} u_{n,t} + P_{wt} + P_{ESS,t} = P_{Dt} \quad (18)$$

where P_{nt} is output of n in t ; $P_{ESS,t}$ is the charge-discharge

power of the lead-acid battery in t (positive during discharging and negative during charging); P_{D_t} is the forecasted load in t ; and P_{w_t} is the forecasted wind power in t .

b) *Output of microturbine*

$$P_n^{\min} u_{n,t} \leq P_{m_t} u_{n,t} \leq P_n^{\max} u_{n,t} \quad (19)$$

where P_n^{\min} and P_n^{\max} are the minimum and maximum output limits of n .

c) *Lead-acid battery*

During charging,

$$S_{oc}(t+1) = S_{oc}(t) + P_t^c \eta_c \Delta t \quad (20)$$

During discharging,

$$S_{oc}(t+1) = S_{oc}(t) - P_t^d \Delta t / \eta_d \quad (21)$$

where $S_{oc}(t+1)$ and $S_{oc}(t)$ are residual capacities of the lead-acid battery in $t+1$ and t , respectively; P_t^c and P_t^d are the charge and discharge power of the lead-acid battery in t ; η_c and η_d are charging and discharging efficiency of the lead-acid battery; and Δt is interval between two periods (It defaults to 1h in this paper).

The rated power limit of the lead-acid battery is:

$$0 \leq P_t^c \leq P_{ch,max} \quad (22)$$

$$0 \leq P_t^d \leq P_{dch,max} \quad (23)$$

where P_t^c and P_t^d are the charge and discharge power of the lead-acid battery in t ; $P_{ch,max}$ and $P_{dch,max}$ are the maximum charge and discharge power.

The residual capacity limit of the lead-acid battery is:

$$S_{ocmin} \leq S_{oc}(t) \leq S_{ocmax} \quad (24)$$

where $S_{oc}(t)$ is residual capacity of the lead-acid battery in t ; S_{ocmin} and S_{ocmax} are the minimum and maximum residual capacity limits of the lead-acid battery.

S_{oc} is fixed at the end of every dispatching cycle:

$$S_{oc}(0) = S_{oc}(T_{end}) = S_{ocinitial} \quad (25)$$

where $S_{oc}(0)$ is residual capacity of the lead-acid battery at beginning of the dispatching cycle; $S_{oc}(T_{end})$ is residual capacity of the lead-acid battery at end of the dispatching cycle; and $S_{ocinitial}$ is the set residual capacity of the lead-acid battery at beginning of the dispatching cycle.

d) *Spinning reserve*

Load and wind output change during microgrid operation. To ensure the safe and reliable operation, it is necessary to equip with certain spinning reserves. Spinning reserves in microgrid (running) are often provided by conventional units and lead-acid battery together.

Spinning reserves in the power system include positive spinning reserve (positive reserve) and negative spinning reserve (negative reserve) [9-10].

The maximum positive reserve provided by conventional unit is:

$$R_{nt}^{up} = \sum_{n=1}^N P_n^{\max} u_{n,t} - \sum_{n=1}^N P_{nt} u_{n,t}, \forall t \quad (26)$$

The maximum positive reserve provided by lead-acid battery is:

$$R_{ESS_t}^{up} = \min \{ \eta_d (S_{oc}(t) - S_{ocmin}) / \Delta t, P_{dch,max} - P_{ESS_t} \}, \forall t \quad (27)$$

The positive reserve capacity provided by the lead-acid battery in t is restricted by the minimum capacity and maximum discharge power of the lead-acid battery simultaneously. If the lead-acid battery is charging in t , it has to reduce charge power and even transits to discharge state in order to smooth wind output and load fluctuations. The maximum reserve provided by the lead-acid battery in t still can be calculated from equation (27).

The maximum negative reserve provided by conventional units is:

$$R_{nt}^{down} = \sum_{n=1}^N P_{nt} u_{n,t} - \sum_{n=1}^N P_n^{\min} u_{n,t}, \forall t \quad (28)$$

The maximum negative reserve provided by lead-acid battery is:

$$R_{ESS_t}^{down} = \min \{ (S_{ocmax} - S_{oc}(t)) / \eta_c / \Delta t, P_{ch,max} - P_{ESS_t} \}, \forall t \quad (29)$$

During the stand-alone microgrid operation, it needs large spinning reserve capacity to smooth all possible wind output and load fluctuations in the whole dispatching cycle. This will increase investment, operating and maintenance costs correspondingly. In fact, power grid seldom suffers extreme operating conditions and such extreme operating condition lasts far shorter than the normal operation. Therefore, we can consider to achieving better economical efficiency at the cost of certain system reliability. In this paper, the spinning reserve capacity was determined by using probabilistic constraints:

$$P \{ -(R_{nt}^{down} + R_{ESS_t}^{down}) \leq R_t \leq R_{nt}^{up} + R_{ESS_t}^{up} \} \geq \alpha \quad (30)$$

$$R_t = \Delta P_{D_t} + \Delta P_{w_t} \quad (31)$$

where R_t is the spinning reserve demand of microgrid in t ; $P\{\}$ is probability; α is confidence level; ΔP_{D_t} is the load forecasting error in t , which is supposed obeying normal distribution^[11] ($\Delta P_{D_t} \sim \mathcal{N}(0, (\sigma_2 \cdot P_{D_t})^2)$); ΔP_{w_t} is the wind forecasting error in t , which is also supposed obeying normal distribution^[12] ($\Delta P_{w_t} \sim \mathcal{N}(0, (\sigma_1 \cdot P_{w_t})^2)$).

Load and wind power were forecasted using methods in Reference [11-12]. Suppose that the independent wind power forecasting error and load forecasting error obey normal distribution and their sum also obey normal distribution^[13] ($R_t \sim \mathcal{N}(0, (\sigma_2 \cdot P_{D_t})^2 + (\sigma_1 \cdot P_{w_t})^2)$).

Equation (30) was solved by using method in Reference [14]. The calculated probability is an approximate estimation.

V. MODEL SOLVING

Solving the established model using particle swarm optimization (PSO).

Step 1: Input unit parameters, wind speed, load and calculating data of load shifting rate. Forecast wind power and load.

Step 2: Generate the initial particle swarm (including N_g random particles). Each particle is a three-dimensional array which is used to store TOU data.

Step 3: Adjust every particle to meet equation (16) and (17).

Step 4: Adjust load by using method in Section II ac-

ording to the TOU data of every particle.

Step 5: Based on the load curve of every particle, use PSO algorithm to solve the established economical operation model of microgrid, calculating C_{total} of every particle and sales revenue of power supply enterprises. Then, $C_{benefit}$ under different TOU policies can be calculated.

Step 6: Based on previous five steps, the objective function of every particle can be calculated. Penalty function method was used in view of purchase cost constraint of users. The fitness function is:

$$Fitness = A - C_{benefit}(x) + B(x) \quad (32)$$

$$B(x) = \begin{cases} 0 & M_0 \geq M_1 \\ \beta & M_0 < M_1 \end{cases} \quad (33)$$

where A is a large positive constant; $C_{benefit}(x)$ is the objective function value of particle x ; $B(x)$ is the penalty term of particle x . The value $B(x)$ is calculated from equation (33). When constraints in equation (13) are not satisfied, $B(x)$ is a large positive constant (β); otherwise, $B(x)=0$.

Step 7: Update locations and speeds of particles. Make cross and mutation operations.

Step 8: Repeat Step3, Step4, Step5, Step6 and Step7 until reaching conditions for iterative convergence.

Step 9: Obtain the optimal TOU as well as output of conventional unit and charge-discharge power of the lead-acid battery in the corresponding dispatching cycle (one day).

The flow chart of PSO algorithm is shown in Fig. 4.

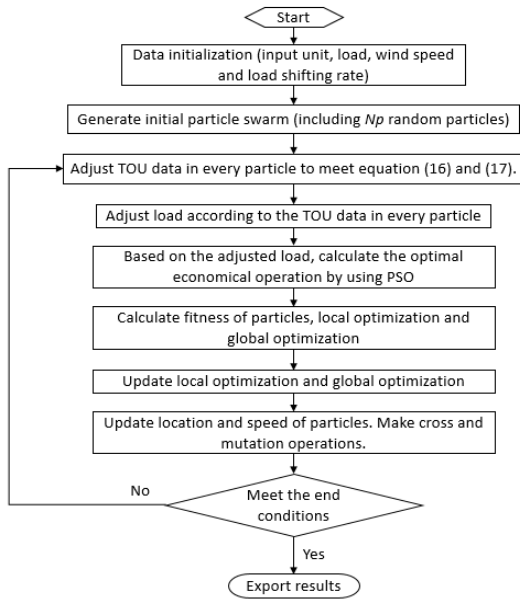


Figure 4. Flow chart of the algorithm of optimal TOU considering demand side response and economical operation of microgrid

VI. CASE STUDY

The case study was conducted using a stand-alone microgrid with 3 microturbines, 2 wind turbines and 1 lead-acid battery. Their parameters are listed in Table 1~3. Residual capacity of lead-acid battery at beginning of dispatching cycle is: $S_{ocinitial}=48$ kWh. Period division: valley: 0:00-7:00 (8h); peak: 10:00~12:00 and

18:00~21:00 (7h); flat: rest 9h.

TABLE I. PARAMETERS OF MICROTURBINE

Type	Power/kW		Set
	Lower limit	Upper limit	
Microturbine 1(MT1)	5	35	1
Microturbine 2(MT2)	10	45	1
Microturbine 3(MT3)	15	65	1

TABLE II. PARAMETERS OF WIND TURBINE

Type	Power /kW		Cut-in wind speed / (m/s)	Cut-out wind speed / (m/s)	Rated wind speed / (m/s)	Set
	Lower limit	Upper limit				
Wind turbine	0	30	3	25	15	2

TABLE III. PARAMETERS OF LEAD-ACID BATTERY

Type	Power /kW		$S_{ocmin}/(kW \cdot h)$	$S_{ocmax}/(kW \cdot h)$	η_c	η_d
	Max charge power	Max discharge power				
Lead-acid battery	40	40	48	160	0.95	0.95

For the testing stand-alone microgrid, the average purchase price before the implementation of TOU is 0.65RMB/ kWh. The optimal TOU calculated by using the established mode is shown in Table 4. $C_{benefit}$ of one day before the implementation of TOU is 587.56 RMB (including $C_{total}=1325.3$ RMB). $C_{benefit}$ of one day under the optimal TOU is 631.70RMB (including $C_{total}=1280.33$ RMB), 7.5% up than that before the implementation of TOU. Moreover, the purchasing cost of users isn't increased. Load curve before and after the implementation of TOU is shown in Fig .5.

TABLE VI. OPTIMAL TOU OF STAND-ALONE MICROGRID

Periods	Price (RMB/kWh)	Shifted loads (kWh)
Peak	0.946	-130.14
Flat	0.606	-27.17
Valley	0.373	157.32

In Fig .5, the load curve after implementation of TOU is much smoother than before. This is caused by load shifting from peak to flat and valley as users' response to TOU. The generation scheduling of stand-alone microgrid before and after TOU implementation is shown in Fig .6 and Fig .7, respectively.

Comparing Fig .6 and Fig .7, we can conclude that:

a) Some loads are shifted from peak to flat and valley as users make responses to TOU, thus smoothing the load curve.

b) Since load fluctuates gently under TOU, the output of MT3 bearing basic load fluctuates gently too, remaining at high output. Due to the lower operating cost of MT3, the operating cost of the stand-alone microgrid is decreased accordingly.

c) With lower load at peak under TOU, the stand-alone microgrid requires smaller spinning reserve capacity and the charge-discharge power of the energy storage device decreases, thus prolonging service life of the energy storage device and reducing operating cost. In actual microgrid considering effect of demand side response, it can reduce installed capacity of energy storage

device appropriately to lower equipment investment cost.

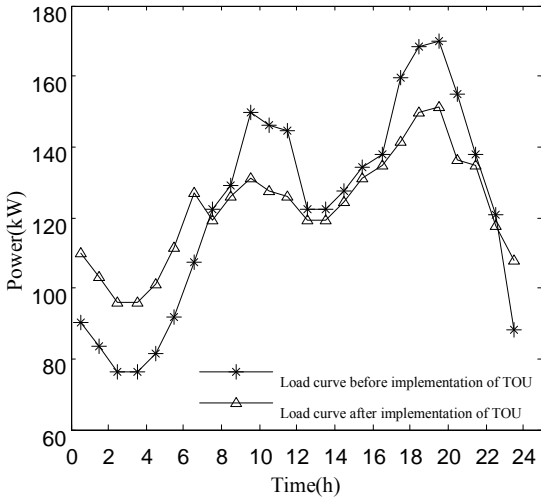


Figure 5. Load curve before and after implementation of TOU

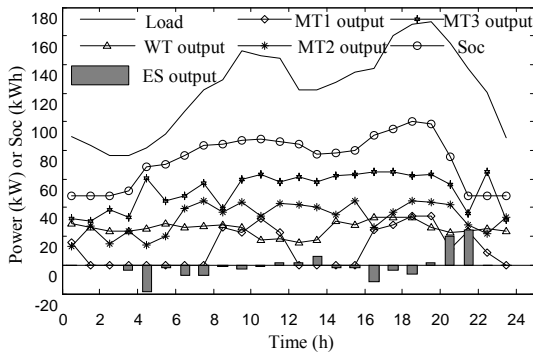


Figure 6. Optimal generation scheduling of stand-alone microgrid under the unifying price

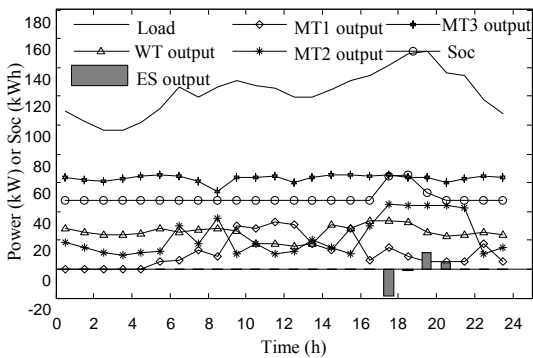


Figure 7. Optimal generation scheduling of stand-alone microgrid under the optimal TOU

VII. CONCLUSIONS

Based on existing associated researches, this paper discusses effect of demand side response on the economical operation of microgrid, establishes the TOU optimization model considering demand side response and economical operation, analyzes effect of users on TOU, and integrates demand side response into generation scheduling of microgrid. TOU can guide users to adjust electricity consumption structure and narrow peak-valley load gap.

The established model is solved using PSO algorithm. Based on a stand-alone microgrid, the optimal TOU and optimal generation scheduling are calculated. Results confirm the feasibility and validity of the established model.

The established model can provide certain reference to short-term scheduling of microgrid in practical engineering. Subsequent researches can improve the optimal economical operation model of microgrid considering demand side response, involve interruptible load and analyze its effect on the economical operation of microgrid, and establish an economical operation model of microgrid considering interaction with purchase price of the main grid.

REFERENCES

- [1] Liu Yan, Tan Zhongfu, Qi Jianxun. "TOU optimization model". Chinese Journal of Management Science, 2005, 13(5):87-92.
- [2] Gao Lin. "Research on the application of TOU decision optimization model based on user response". Hefei: Hefei University of Technology, 2010.
- [3] Wang Mianbin, Tan Zhongfu, Zhang Rong, et al. "Optimization model of TOU and electricity distribution for generation side". Electric Power Automation Equipment, 2007, 27(8):16-21.
- [4] Wu Xiong, Wang Xiuli, Cui Qiang. "Optimal economical operation of microgrid considering demand side management". Journal of Xi'an Jiaotong University, 2013, 47(6): 90-96.
- [5] Tan Zhongfu, Chen Guangjuan, Zhao Jianbao, et al. "Energy-saving dispatching-oriented joint optimization model of TOU for generation side and selling side". Proceedings of the CSEE, 2009, 29(1): 55-62.
- [6] Palma-Behnke R, Benavides C, Aranda E, et al. "Energy management system for a renewable based microgrid with a demand side management mechanism". Computational Intelligence Applications In Smart Grid (CIASG), 2011:1-8.
- [7] Liu Xiacong, Wang Beibei, Li Yang, et al. "Power dispatching model in smart power grids one day before generation considering user interaction". Proceedings of the CSEE, 2013, 33(1): 30-38.
- [8] Ruan Wenjun, Wang Beibei, Li Yang, et al. "Research on user response behaviors under TOU". Power System Technology, 2012, 36(7):86-93.
- [9] Lee T Y. "Optimal spinning reserve for a wind-thermal power system using EIPSO". IEEE Transactions on Power Systems, 2007, 22(4): 1612-1621.
- [10] Zhang Haifeng, Gao Feng, Wu jiang, et al. "A dynamic economic dispatching model for power grid containing wind power generation system". Power System Technology, 2013, 37(5):1198-1303(in Chinese).
- [11] Hanmandlu M, Chauhan B K. "Load forecasting using hybrid models". IEEE Transactions on Power Systems, 2011, 26(1):20-29.
- [12] Meng Yangyang, Lu Jiping, Sun Huali, et al. "Short-term wind power forecasting based on similar days and artificial neural network". Power System Technology, 2010, 34(12): 163-168(in Chinese).
- [13] Sheng Zhou, Xie Shiqian, Pan Chengyi. "Probability and mathematical statistics". Beijing: Higher Education Press, 2005: 90-98.
- [14] LI W. "Risk assessment of power systems: models, methods and applications". Piscataway, New Jersey, USA: Wiley-IEEE Press, 2005: 242-243.